(12)

SDAC-TR-76-5

EVALUATION OF THE KOREAN SHORT-PERIOD ARRAY

MAURICE BLAIK AND ZOLTAN DER
Seismic Data Analysis Center
Teledyne Geotech, 314 Montgomery Street, Alexandria, Virginia 22314

20 APRIL 1976

APPROVED FOR PUBLIC RELEASE; DISTRIBUTION UNLIMITED.

Sponsored By
The Defense Advanced Research Projects Agency
Nuclear Monitoring Research Office
1400 Wilson Boulevard, Arlington, Virginia 22209
ARPA Order No. 1620

Monitored By
VELA Seismological Center
312 Montgomery Street, Alexandria, Virginia 22314

Unclassified

SECURITY CLASSIFICATION OF THIS PAGE (When Data Entered)

14

REPORT DOCUMENTATION PAGE

READ INSTRUCTIONS BEFORE COMPLETING FORM

1. REPORT NUMBER SDAC-TR-76-5	2. GOVT ACCESSION NO.
	3. RECIPIENT'S CATALOG NUMBER 9
4. TITLE (and Subtitle) 6 EVALUATION OF THE KOREAN SHORT-PERIOD ARRAY.	5. TYPE OF REPORT & PERIOD COVERED Technical rept.,
	6. PERFORMING ORG. REPORT NUMBER 15
7. AUTHOR(s) Blaik, Maurice and Der, Zoltan	8. CONTRACT OR GRANT NUMBER(s) F08606-76-C-0004, ARPA Order-1620
9. PERFORMING ORGANIZATION NAME AND ADDRESS Teledyne Geotech 314 Montgomery Street Alexandria, Virginia 22314	10. PROGRAM ELEMENT, PROJECT, TASK AREA & WORK UNIT NUMBERS VT/6709
11. CONTROLLING OFFICE NAME AND ADDRESS Defense Advanced Research Projects Agency Nuclear Monitoring Research Office 1400 Wilson Blvd.-Arlington, Virginia 22209	11 12. REPORT DATE 20 Apr 1976
	13. NUMBER OF PAGES 38
14. MONITORING AGENCY NAME & ADDRESS(if different from Controlling Office) VELA Seismological Center 312 Montgomery Street Alexandria, Virginia 22314 12 42p.	15. SECURITY CLASS. (of this report) Unclassified
	15a. DECLASSIFICATION/DOWNGRADING SCHEDULE

16. DISTRIBUTION STATEMENT (of this Report)

APPROVED FOR PUBLIC RELEASE; DISTRIBUTION UNLIMITED.

10 Maurice /Blaik Zoltan /Der

17. DISTRIBUTION STATEMENT (of the abstract entered in Block 20, if different from Report)

18. SUPPLEMENTARY NOTES

19. KEY WORDS (Continue on reverse side if necessary and identify by block number)

Seismic Arrays
Beamforming
m_b Thresholds

20. ABSTRACT (Continue on reverse side if necessary and identify by block number)

The Korean Seismic Research Station (KSRS) short-period array was evaluated using data which cover eight-hour time periods daily between May and June 1973. Most of the data is of poor quality due to instrumental problems. The average noise reduction obtained by beaming was about 2 dB better than $\sqrt{N}$ due to the almost continuous presence of propagating coherent noise at the station. The 50% detection body wave magnitude threshold was
square root of (N)

OVER

DD FORM 1 JAN 73 1473 EDITION OF 1 NOV 65 IS OBSOLETE

Unclassified

SECURITY CLASSIFICATION OF THIS PAGE (When Data Entered)

408258

1B

cont'd

found to be 4.35 $\pm$ .45 (95% confidence interval) at the epicentral distance of 60. The 90% detection threshold was found to be 5.42 $\pm$ .45 magnitude units.

Jag

(+ or -

EVALUATION OF THE KOREAN SHORT-PERIOD ARRAY

SEISMIC DATA ANALYSIS CENTER REPORT NO.: SDAC-TR-76-5

AFTAC Project Authorization No.:	VELA T/6709/B/ETR
Project Title:	Seismic Data Analysis Center
ARPA Order No.:	2551
ARPA Program Code No.:	6F10
Name of Contractor:	TELEDYNE GEOTECH
Contract No.:	F08606-76-C-0004
Date of Contract:	01 July 1975
Amount of Contract:	$2,319,926
Contract Expiration Date:	30 June 1976
Project Manager:	Royal A. Hartenberger (703) 836-3882

P. O. Box 334, Alexandria, Virginia 22314

ABSTRACT

The Korean Seismic Research Station (KSRS) short-period array was evaluated using data which cover eight-hour time periods daily between May and June 1973. Most of the data is of poor quality due to instrumental problems. The average noise reduction obtained by beaming was about 2 dB better than $\sqrt{N}$ due to the almost continuous presence of propagating coherent noise at the station. The 50% detection body wave magnitude threshold was found to be $4.35 \pm .45$ (95% confidence interval) at the epicentral distance of 60°. The 90% detection threshold was found to be $5.42 \pm .45$ magnitude units.

TABLE OF CONTENTS

LIST OF FIGURES

LIST OF TABLES

INTRODUCTION

This report presents the results of evaluation of a limited sample of digital data from the Korean Seismic Research Station (KSRS). The data consists of 45 digital tapes, with one eight-hour time interval on each tape, and covers the three-month period of May, June and July in 1973. Table 1 gives the dates, time windows and tape numbers for all of the tapes. The three most important observations about the list of 45 tapes are that (1) the eight-hour intervals every other day provide samples for only one-sixth of the total three-month interval, (2) the time of year is limited to late spring and early summer, and (3) the time of day represented by different tapes is highly variable and provides samples for all hours both day and night, although on different days. This implies that diurnal noise variation may be observable, but seasonal variations cannot be observed.

Table 2 gives the list of events from the NEIS bulletin that fall within the time windows contained on the 45 data tapes. The events are distributed around the world in the principal seismic regions. The asterisked events were detected. The nine regions of best sampling on this list are (in order of decreasing sample size) Chile, Kuriles, Alaska, Fijis, Hokkaido, New Guinea, Nevada, Mexico, and New Hebrides. The first, Chile, is represented by 19 events and the last, New Hebrides, contains 5 events.

The Korean short-period array is centered about 150 km east of Seoul, South Korea. It consists of 19 seismometers in the configuration shown in Figure 1. They are located in a pattern of two rings around one central instrument. The numbers shown are the tape channel locations for each seismometer site, and it can be seen that number four is the only one located about halfway between two rings. The diameter of the two rings are 4.25 and 9 km . The greatest spacing of any two pair of instruments is 10 km (between Nos. 11 and 17), and the smallest spacing is 1.5 km (between Nos. 4 and 13). Three principal directional alignments are emphasized in Figure 1. These are 013° (193°), 084° (264°), and 135° (315°).

TABLE I

KSRS Data Tape Time Windows

	KSRS	SDAC #	DATE	START TIME	# EVENTS RUN	# OF SIGNALS OBSERVED	DATE	STOP TIME
1	205	(L21957)	Apr 29	00 36 56	7	5	Apr 29	08 34 47
2	212	(21958) Bad Tape	May 1	08 40 07	0	0	May 1	16 40 19
3	217	(21959)	May 3	00 44 07	7	0	May 3	08 42 43
4	223	(21960)	May 5	00 55 37	6	0	May 5	08 53 34
5	229	(21961)	May 7	00 54 13	2	4	May 7	08 51 55
6	235	(21962)	May 9	00 53 28	1	0	May 9	08 50 55
7	241	(21963)	May 11	00 48 46	0	0	May 11	08 46 01
8	247	(21964)	May 13	00 50 22	3	2	May 13	08 48 31
9	254	(21965)	May 15	10 38 30	5	0	May 15	18 42 21
10	259	(21966)	May 17	04 04 48	2	2	May 17	12 02 57
11	266	(21967)	May 19	11 54 06	2	2	May 19	19 56 15
12	272	(21968)	May 21	11 54 15	2	1	May 21	19 56 39
13	278	(21969)	May 23	12 19 26	1	0	May 23	20 17 44
14	285	(21970)	May 25	07 07 55	5	3	May 25	15 04 07
15	292	(21971)	May 27	08 14 16	2	0	May 27	16 21 54
16	298	(21972)	May 29	11 15 23	5	4	May 29	19 12 17
17	304	(21973)	May 31	09 59 44	3	2	May 31	17 58 40
18	310	(21974)	Jun 2	09 47 47	1	1	Jun 2	17 45 02
19	316	(21975)	Jun 4	09 44 24	7	3	Jun 4	17 41 21
20	322	(21976)	Jun 6	11 07 21	7	4	Jun 6	19 04 33
21	328	(21977)	Jun 8	11 09 24	5	2	Jun 8	19 06 03
22	334	(21978)	Jun 10	11 06 42	5	3	Jun 10	19 03 06
23	339	(21979)	Jun 12	08 48 39	4	3	Jun 12	16 45 05
24	345	(21980)	Jun 14	08 36 24	4	3	Jun 14	15 48 45
25	351	(21981)	Jun 16	07 39 24	7	3	Jun 16	15 38 48
26	358	(21982)	Jun 18	12 02 29	6	4	Jun 18	19 56 59
27	365	(21983)	Jun 20	14 30 44	3	2	Jun 20	22 23 08
28	371	(21984)	Jun 22	14 13 25	5	4	Jun 22	22 10 34
29	377	(21985)	Jun 24	13 58 55	8	6	Jun 24	21 53 28
30	383	(21986)	Jun 26	13 40 43	5	3	Jun 26	21 34 19
31	389	(21987)	Jun 28	13 51 04	8	6	Jun 28	21 41 22
32	395	(21988)	Jun 30	06 32 53	5	1	Jun 30	14 26 41
33	401	(21989)	Jul 2	05 56 24	7	4	Jul 2	14 51 33
34	408	(21990)	Jul 4	12 03 38	6	3	Jul 4	19 57 08
35	413	(21991)	Jul 6	04 45 47	6	5	Jul 6	12 49 32
36	420	(21992)	Jul 8	12 24 04	5	3	Jul 8	20 39 22
37	426	(21993)	Jul 10	12 45 53	3	2	Jul 10	20 42 32
38	432	(21994)	Jul 12	12 59 26	8	5	Jul 12	20 56 11
39	438	(21995)	Jul 14	12 37 20	2	2	Jul 14	20 34 17
40	444	(21996)	Jul 16	12 17 41	4	3	Jul 16	20 13 08
41	449	(21997)	Jul 18	05 12 15	3	0	Jul 18	13 12 00
42	456	(21998)	Jul 20	09 36 16	5	1	Jul 20	18 36 20
43	462	(21999)	Jul 22	13 39 34	8	4	Jul 22	21 40 34
44	468	(22000)	Jul 24	13 23 19	7	3	Jul 24	21 23 25
45	474	(22001)	Jul 26	13 31 40	7	6	Jul 26	21 30 16

TABLE II

NEIS Events Listed During Times Covered by Data Tapes

	GEOGRAPHIC LOCATION	DATE	ORIGIN HR MN SECS	LOCATION LAT	LOCATION LONG	DEPTH KM	MAG MBD	
*1	Near E Coast Honshu, Japan	4-29	00 37 38.3	39.246N	142.407E	33	4.3	
*2	Banda Sea	4-29	00 59 33.8	6.323S	129.874E	126	5.3	
*3	Philippine Islands Region	4-29	02 03 56.1	19.727N	120.904E	33N	4.5	+
*4	South of Panama	4-29	03 45 25.3	4.919N	78.160W	33N	4.4	+
5	Andrean Is. Aleutians	4-29	04 55 10.4	50.806N	178.699W	33	3.7	
6	New Britain Region	4-29	06 27 11.4	6.197S	150.189E	56	0.0	
*7	Hokkaido, Japan, Region	4-29	07 33 59.6	41.705N	142.689E	50	3.8	
8	Ionian Sea	5-03	01 22 33.3	38.109N	19.771E	32	4.0	
9	South of Fiji Islands	5-03	02 23 11.5	25.383S	179.796W	399	4.2	
10	Tanzania	5-03	02 27 13.0	8.452S	32.759E	33N	4.5	
11	Near East Coast Kamchatka	5-03	04 36 37.7	50.978N	157.809E	33N	4.4	
12	Fiji Islands Region	5-03	04 37 15.0	16.273S	176.613W	429	4.3	
13	Queen Elizabeth Islands	5-03	05 42 34.1	76.604N	107.411W	33N	4.3	
14	Southern Iran	5-03	07 44 24.4	28.202N	51.904E	41	4.6	
*15	Solomon Islands	5-05	01 35 19.5	8.151S	156.408E	15	5.4	
16	Hokkaido, Japan, Region	5-05	03 37 13.6	41.852N	145.544E	53	4.2	
17	Near E Coast Honshu, Japan	5-05	03 52 26.4	37.129N	141.323E	41D	5.4	+
18	Near E Coast Honshu, Japan	5-05	05 12 23.3	36.154N	140.063E	80	4.8	+
*19	Iran	5-05	06 12 35.6	33.341N	57.384E	33N	4.6	
*20	Honshu, Japan	5-05	07 40 58.1	40.886N	140.306E	17	5.1	
21	Aegean Sea	5-05	08 09 44.5	39.018N	23.414E	33N	3.6	
22	Aegean Sea	5-05	08 21 03.0	39.016N	23.437E	26	3.6	
*23	Hokkaido, Japan, Region	5-05	08 46 35.5	42.707N	142.363E	106	3.8	
24	Santa Cruz Islands Region	5-07	01 16 42.5	10.863S	164.535E	33N	4.7	
25	South of Panama	5-07	04 29 41.9	4.830N	78.166W	59	4.4	+
26	Peru-Bolivia Border Region	5-09	04 06 40.3	17.867S	69.200W	154	3.7	+
27	California-Arizona Border	5-09	11 53 51.3	34.200N	116.183W	8	0.0	
*28	North of Ascension Island	5-13	01 32 36.1	0.934S	13.189W	33N	5.3	+
*29	Bonin Islands Region	5-13	04 47 29.8	28.312N	139.389E	452	4.2	
30	Off Coast of North California	5-13	06 12 01.5	41.896N	126.720W	33N	4.5	
31	New Hebrides Islands	5-15	12 53 50.2	17.760S	167.551E	18	4.7	
32	New Hebrides Islands	5-15	15 08 28.3	17.642S	167.642E	33N	0.0	

TABLE II (Continued)

NEIS Events Listed During Times Covered by Data Tapes

	GEOGRAPHIC LOCATION	DATE	ORIGIN HR	MN	SECS	LOCATION LAT	LONG	DEPTH KM	MAG MBD	
33	Nevada	5-15	15	21	01.5	37.975N	114.725W	10G	0.0	
34	Fiji Islands Region	5-15	16	19	54.3	17.743S	178.493W	570	4.7	
35	Central California	5-15	17	18	50.7	35.100N	117.483W	8	0.0	
*36	Kurile Islands	5-17	06	17	46.4	44.575N	149.163E	33N	5.1	
*37	Southern Sinkiang Province	5-17	09	38	09.9	41.025N	82.195E	33N	5.5	
*38	South of Mariana Islands	5-19	17	57	05.8	12.125N	143.731E	71	4.6	
*39	Southern Peru	5-19	18	18	31.4	15.575S	73.849W	79D	5.2	+
*40	Carlsberg Ridge	5-21	11	50	20.5	1.259S	67.486E	33N	5.0	
41	Near Coast Guerrero, Mexico	5-12	15	25	20.2	16.895N	99.292W	96	4.8	+
42	Windward Islands	5-21	16	51	47.2	11.006N	61.345W	33N	3.9	+
43	Central Alaska	5-23	17	48	59.0	63.986N	150.717W	34	3.8	
*44	West Pakistan	5-25	08	39	53.9	25.536N	66.498E	57	4.9	
45	Near Coast of Central Chile	5-25	09	45	12.1	34.165S	72.095W	25	4.3	+
*46	Off Coast of Oregon	5-25	11	36	25.9	43.345N	126.767W	33N	4.2	
*47	South of Alaska	5-25	13	17	26.1	53.204N	161.281W	39	4.9	
48	Mississippi	5-25	14	40	13.9	33.917N	90.775W	6	0.0	+
49	Malawi	5-27	09	26	00.7	10.379S	34.294E	33N	4.4	
50	Southern Nevada	5-27	10	12	40.8	36.854N	114.927W	5G	0.0	
*51	Mascarene Islands Region	5-29	11	46	54.6	17.453S	66.495E	33N	4.8	
*52	South Sandwich Island Region	5-29	13	14	06.1	57.872S	25.384W	75	4.8	+
53	Northern Chile	5-29	13	25	17.7	22.266S	68.582W	111D	4.8	
*54	Baffin Island Region	5-29	16	06	39.2	71.896N	75.901W	33N	4.1	
*55	Peru-Prazil Border Region	5-29	16	38	44.8	8.467S	73.966W	192	4.6	+
*56	Northern Sumatra	5-31	12	22	02.8	4.400N	96.329E	33N	4.3	
57	Gulf of Alaska	5-31	14	35	18.7	58.104N	148.711W	33N	3.6	
*58	Rat Islands, Aleutians	5-31	17	36	52.9	51.339N	176.301E	10	4.8	
*59	Southern Iran	6-02	13	42	09.1	26.945N	53.433E	33N	3.9	
*60	Philippine Islands Region	6-04	09	57	08.4	6.023N	127.115E	84	4.4	
*61	New Britain Region	6-04	13	02	38.0	5.817S	151.266E	77	4.7	
*62	Ecuador	6-04	13	14	29.8	1.312S	77.792W	177	4.3	+
63	Near E. Coast of E. Russia	6-04	15	34	39.8	46.643N	140.847E	33N	4.6	
64	Near N. Coast of W. New Guinea	6-04	15	47	52.4	2.511S	139.102E	33N	0.0	
65	Near Islands, Aleutians	6-04	16	21	22.8	51.578N	174.610E	48	4.5	
66	Hokkaido, Japan, Region	6-06	11	49	29.3	43.230N	145.793E	58	4.3	
*67	Southern Nevada	6-06	13	00	00.1	37.245N	116.346W	0	6.1	
68	New Britain Region	6-06	13	19	49.5	6.184S	151.866E	36	4.8	
*69	Solomon Islands	6-06	13	59	12.1	7.714S	156.478E	59	0.0	

TABLE II (Continued)

NEIS Events Listed During Times Covered by Data Tapes

	GEOGRAPHIC LOCATION	DATE	ORIGIN HR	MN	SECS	LOCATION LAT	LONG	DEPTH KM	MAG MBD	
*70	Hindu Kush Region	6-06	15	51	17.1	36.325N	70.640E	220	5.1	
*71	Northern Celebes	6-06	16	43	42.4	0.639N	121.914E	102	5.0	+
72	Off Coast of Oregon	6-06	17	22	22.1	43.417N	126.106W	33N	4.5	
73	New Hebrides Islands	6-06	18	01	17.8	17.498S	167.749E	21	4.9	
*74	Bonin Islands Region	6-08	11	54	08.9	28.164N	142.551E	33N	4.3	
*75	New Guinea	6-08	13	45	26.0	4.503S	143.564E	146	4.6	
76	Kamchatka	6-08	17	17	50.8	54.970N	159.417E	33N	4.3	
77	Southern Iran	6-08	17	56	59.1	26.462N	61.115E	33N	4.6	
78	Guerrero, Mexico	6-08	18	05	35.3	18.039N	100.456W	107	4.3	+
79	Off Coast of Mexico	6-10	12	39	18.5	14.409N	105.423W	33N	4.4	+
*80	Celebes Sea	6-10	15	55	22.6	3.518N	124.272E	329	4.6	+
81	Southern Sinkiang Province	6-10	16	08	42.2	39.530N	74.813E	33N	5.2	
*82	Carlsberg Ridge	6-10	16	42	14.5	1.365S	67.305E	33N	4.6	
*83	Guatemala	6-10	17	35	53.9	14.203N	91.402W	92	4.6	+
84	Crete	6-12	11	01	52.6	34.215N	26.191E	54	4.3	
*85	Solomon Islands	6-12	12	21	30.2	6.648S	154.868E	47	4.9	
*86	Off East Coast Kamchatka	6-12	14	21	24.2	53.625N	161.590E	33N	5.4	
*87	Hokkaido, Japan, Region	6-12	15	24	42.1	41.607N	139.211E	199	4.8	
88	Mozambique	6-14	09	34	19.5	20.842S	35.612E	33N	0.0	+
*89	Flores Sea	6-14	11	02	46.9	7.291S	120.385E	631D	5.8	+
*90	North of Severnaya Zemlya	6-14	12	49	16.2	84.135N	113.769E	33N	4.5	
*91	Sumba Island Region	6-14	14	49	48.3	10.190S	120.530E	33N	5.6	+
92	Kenai Peninsula, Alaska	6-16	07	34	44.9	60.349N	151.710W	82	0.0	
93	Central Alaska	6-16	07	50	45.2	64.731N	147.224W	7	0.0	
94	Fiji Islands Region	6-16	11	53	07.5	19.252S	177.916W	525G	4.3	
*95	Lake Baikal Region	6-16	12	12	32.2	55.002N	112.571E	33N	4.5	
96	Southern Nevada	6-16	14	36	43.6	37.239N	116.337W	2	0.0	
*97	Off Coast of Oregon	6-16	14	43	47.5	44.980N	125.774W	33N	5.6	
*98	Banda Sea	6-16	15	04	51.4	5.944S	130.650E	122	5.1	
*99	Hokkaido, Japan, Region	6-18	13	13	51.0	42.638N	145.825E	35G	4.8	
*100	Kurile Islands	6-18	14	29	39.2	43.543N	146.952E	33N	4.5	
*101	Kurile Islands	6-18	14	31	39.8	43.419N	147.126E	36D	4.7	
102	Bonin Islands Region	6-18	15	55	34.4	27.857N	142.104E	48	4.9	
103	Off Coast Hokkaido, Japan	6-18	17	45	43.7	42.498N	145.969E	29D	5.8	
*104	Hokkaido, Japan, Region	6-18	18	24	19.6	42.308N	145.411E	29D	5.3	
*105	Off E Coast Honshu, Japan	6-20	14	30	40.9	40.035N	145.671E	35	4.7	

TABLE II (Continued)

NEIS Events Listed During Times Covered by Data Tapes

	GEOGRAPHIC LOCATION	DATE	ORIGIN HR	MN	SECS	LOCATION LAT	LONG	DEPTH KM	MAG MBD	
106	Southern Alaska	6-20	16	59	38.8	60.503N	145.222W	33N	0.0	
*107	Kermadec Islands Region	6-20	18	29	56.2	28.504S	176.648W	52	4.6	
*108	Fiji Islands Region	6-22	17	16	47.5	17.005S	175.795E	16	5.3	
109	California-Nevada Border	6-22	17	20	50.3	37.114N	116.955W	5G	0.0	
*110	New Hebrides Islands	6-22	18	08	22.7	15.319S	166.311E	33N	4.8	
*111	Mariana Islands Region	6-22	18	47	36.6	21.944N	142.895E	269	5.2	
*112	Tonga Islands	6-22	19	51	40.5	21.166S	174.263W	33N	5.5	
113	Near Coast of Central Chile	6-24	16	08	46.5	32.632S	71.748W	46	3.9	+
*114	Mariana Islands Region	6-24	17	15	10.4	21.013N	143.140E	33N	5.5	
*115	Kurile Islands	6-24	17	49	25.4	43.183N	146.404E	40D	4.9	
*116	West New Guinea Region	6-24	17	58	49.8	0.908S	130.629E	65	5.2	
*117	Kurile Islands	6-24	18	41	49.3	43.062N	146.946E	36D	5.2	
*118	Kurile Islands	6-24	20	00	16.1	43.297N	146.800E	51D	5.1	
*119	Norwegian Sea	6-24	21	06	41.3	62.464N	2.123E	33N	0.0	
120	Fiji Islands Region	6-24	21	36	54.2	20.723S	178.801W	624	4.2	
121	Southern Alaska	6-26	14	41	30.8	60.076N	153.405W	129	0.0	
*122	Kurile Islands	6-26	18	02	24.1	43.018N	147.110E	39D	5.6	
*123	Hokkaido, Japan, Region	6-26	18	16	33.1	43.768N	145.707E	43	4.4	
*124	Crete	6-26	19	05	21.9	34.338N	26.134E	38	4.8	
125	Gulf of Alaska	6-26	21	11	06.0	59.459N	145.064W	33N	3.7	
*126	Santa Cruz Islands	6-28	14	11	03.0	12.792S	166.685E	146	5.5	
*127	Molucca Passage	6-28	14	32	56.0	1.347N	125.746E	33N	0.0	
*128	Northern Chile	6-28	15	26	40.2	23.863S	68.830W	94	4.7	+
129	Near Coast of Central Chile	6-28	16	42	06.5	33.799S	71.554W	62	4.1	+
*130	West New Guinea Region	6-28	17	14	17.1	3.191S	134.415E	63	5.2	
*131	Southern Nevada	6-28	19	15	12.4	37.418N	116.086W	0	4.9	
132	Southern Nevada	6-28	19	45	00.5	37.096N	116.001W	5G	0.0	
*133	Banda Sea	6-28	20	23	01.7	5.453S	131.485E	33N	5.4	
*134	Near Coast of Guatemala	6-30	08	08	57.6	13.763N	90.935W	78	5.1	+
135	Tonga Islands Region	6-30	10	04	15.8	17.244S	172.490W	33N	4.5	
136	Near Coast of Chiapas, Mexico	6-30	11	45	56.9	14.947N	93.202W	109	4.2	+
137	West New Guinea Region	6-30	13	23	10.3	3.835S	131.108E	33N	5.2	
138	West New Guinea Region	6-30	13	30	11.7	3.811S	131.379E	33N	4.8	
139	Near Coast of Northern Chile	7-02	09	50	28.0	27.647S	71.677W	19	4.1	+
140	Switzerland	7-02	11	01	26.7	46.736N	6.798E	33N	0.0	
*141	Aegean Sea	7-02	12	14	08.3	39.685N	23.964E	33N	4.2	
*142	Tadzhik SSR	7-02	12	48	25.9	37.774N	72.171E	33N	4.6	

TABLE II (Continued)

NEIS Events Listed During Times Covered by Data Tapes

	GEOGRAPHIC LOCATION	DATE	ORIGIN HR	MN	SECS	LOCATION LAT	LONG	DEPTH KM	MAG MBD	
*143	Southeastern Alaska	7-02	13	36	52.6	57.937N	136.928W	33N	3.8	
144	Kenai Peninsula, Alaska	7-02	14	10	39.9	60.871N	151.018W	33N	0.0	
*145	Near East Coast Kamchatka	7-02	14	36	00.7	53.405N	159.591E	33N	4.2	
146	California-Nevada Border	7-04	12	25	40.1	37.399N	118.561W	5G	0.0	
147	Off East Coast Honshu, Japan	7-04	13	05	46.0	37.874N	141.977E	53	4.0	+
*148	Southeastern Alaska	7-04	13	26	20.3	58.014N	137.854W	33N	4.6	
149	Off Coast of Oregon	7-04	14	17	09.8	44.735N	129.395W	33N	4.5	
*150	India-China Border Region	7-04	16	44	11.4	27.240N	92.474E	26	5.2	
*151	Honshu, Japan	7-04	17	26	24.9	36.260N	139.746E	69	4.2	+
*152	Near Coast of Nicaragua	7-06	05	21	49.1	11.962N	87.588W	51	4.8	+
153	Near Coast of N. Chile	7-06	05	26	08.5	27.029S	71.001W	33N	4.0	+
*154	Chile-Bolivia Border Region	7-06	07	23	31.1	21.854S	68.182W	123	4.3	+
*155	Near Coast of Northern Chile	7-06	09	27	30.7	27.235S	71.142W	34	5.4	+
*156	Near Coast of Northern Chile	7-06	10	58	40.0	27.195S	70.902W	25	4.7	+
*157	Near Coast of Northern Chile	7-06	11	59	30.9	27.447S	70.907W	39	5.0	+
158	Northern Italy	7-08	13	44	31.7	44.390N	9.793E	33N	0.0	
*159	Sea of Okhotsk	7-08	15	16	58.7	47.658N	145.600E	370	3.7	
*160	Leeward Islands	7-08	16	59	08.1	15.914N	60.708W	19D	5.1	+
*161	Near Coast of Northern Chile	7-08	18	12	07.6	26.986S	70.956W	19	5.3	+
162	Near East Coast of Kamchatka	7-08	18	54	23.5	53.813N	160.444E	33N	4.7	
*163	Near Coast of Northern Chile	7-10	15	06	00.4	27.069S	71.196W	22	5.4	+
164	Near Coast of Northern Chile	7-10	17	02	35.1	27.053S	71.149W	28	4.2	+
*165	Kurile Islands	7-10	17	43	15.5	43.576N	146.593E	44	4.0	
166	Volcano Islands Region	7-12	12	57	12.9	22.096N	143.204E	176D	4.2	
167	Near Coast of Northern Chile	7-12	13	45	30.3	27.075S	71.225W	20	5.5	+
168	Union of South Africa	7-12	14	46	07.2	26.031S	27.278E	2	0.0	+
*169	Near Coast of Northern Chile	7-12	15	11	11.5	26.785	70.825W	33N	4.2	
*170	Near Coast of Northern Chile	7-12	15	41	39.3	27.245S	71.452W	15	5.4	
*171	Near Coast of Northern Chile	7-12	15	48	38.8	27.134S	71.169W	33	5.1	
*172	Near Coast of Northern Chile	7-12	16	25	11.9	26.954S	71.131W	31	4.2	
*173	Samar, Philippine Island	7-12	19	10	23.5	12.232N	125.464E	33N	5.2	+
*174	Southern Greece	7-14	12	38	18.3	37.898N	21.072E	36	4.7	
*175	Tibet	7-14	13	39	30.0	35.256N	86.602E	33N	5.9	
*176	Flores Sea	7-16	13	08	27.1	7.463S	122.118E	392	5.4	+
177	Malawi	7-16	18	08	20.0	10.525S	34.270E	33N	4.4	
*178	Guerrero, Mexico	7-16	18	12	57.5	17.323N	100.679W	44	5.6	+

TABLE II (Continued)

NEIS Events Listed During Times Covered by Data Tapes

		GEOGRAPHIC LOCATION	DATE	ORIGIN HR	MN	SECS	LOCATION LAT	LONG	DEPTH KM	MAG MBD	
*	179	Tibet	7-16	19	45	38.2	35.071N	87.450E	15	5.4	+
	180	Near Coast of Northern Chile	7-18	05	19	24.8	25.450S	70.306W	54	4.2	+
	181	Caribbean Sea	7-18	06	55	33.7	17.629N	81.599W	33N	4.6	
	182	Kermadec Islands	7-18	06	58	08.3	29.938S	177.892W	57	4.3	
*	183	Ceram	7-20	10	14	05.6	3.154S	129.925E	33N	4.8	
	184	Turkey	7-20	10	42	24.0	40.265N	29.217E	10G	0.0	
	185	Off Coast of Jalisco, Me.	7-20	13	11	00.4	18.757N	106.545W	33N	4.7	+
	186	Off Coast of Jalisco, Me.	7-20	13	49	31.8	19.093N	106.313W	33N	4.5	+
	187	Off Coast of Jalisco, Me.	7-20	14	26	50.0	18.585N	106.347W	33N	4.1	+
*	188	South Sandwich Island Region	7-22	14	37	35.6	58.765S	25.024W	33N	4.8	+
*	189	Kermadec Islands Region	7-22	15	11	25.6	30.516S	179.329W	261	4.5	
*	190	Mindanao, Philippine Islands	7-22	15	27	01.5	6.317N	124.022E	33N	5.1	+
	191	Afghanistan-USSR Border	7-22	15	59	27.4	36.516N	71.159E	217	3.7	
	192	Banda Sea	7-22	16	44	54.7	6.937S	130.136E	155	0.0	
*	193	South of Honshu, Japan	7-22	18	18	18.3	29.575N	143.046E	33N	4.1	
	194	France	7-22	21	06	56.8	48.396N	6.446E	12	0.0	
	195	Near Coast of Northern Calif.	7-24	13	48	50.7	39.103N	123.162W	6	4.3	
	196	Southern Alaska	7-24	13	50	41.2	61.607N	147.426W	33N	0.0	
*	197	Kurile Islands	7-24	14	50	22.5	43.167N	146.332E	58	4.7	
*	198	Solomon Islands	7-24	15	04	51.4	8.710S	160.797E	64	4.7	
*	199	Near Coast of Central Chile	7-24	20	03	35.3	30.526S	71.601W	60	5.6	+
	200	Off E Coast Honshu, Japan	7-24	20	14	11.3	34.686N	141.885E	59	4.0	+
	201	South of Africa	7-24	20	49	50.6	52.612S	25.882E	31D	4.5	+
*	202	West of MacQuarie Island	7-26	13	39	15.8	52.801S	140.040E	33N	5.6	
*	203	Andaman Islands Region	7-26	14	14	14.4	10.586N	94.064E	33N	4.4	
	204	Kyushu, Japan	7-26	14	45	46.5	32.018N	130.666E	89	4.0	
*	205	Andaman Islands Region	7-26	14	51	33.0	10.280N	93.916E	33N	4.2	
	206	New Ireland Region	7-26	18	20	57.1	5.254S	153.785E	96	0.0	
*	207	Andaman Islands Region	7-26	19	25	25.1	10.371N	94.320E	33N	4.5	
*	208	Andaman Islands Region	7-26	19	35	26.4	10.412N	95.083E	33N	4.2	
*	209	Andaman Islands Region	7-26	20	06	33.2	10.472N	93.893E	33N	5.1	

* These events were detected at KSRS

+ These events are off-beam

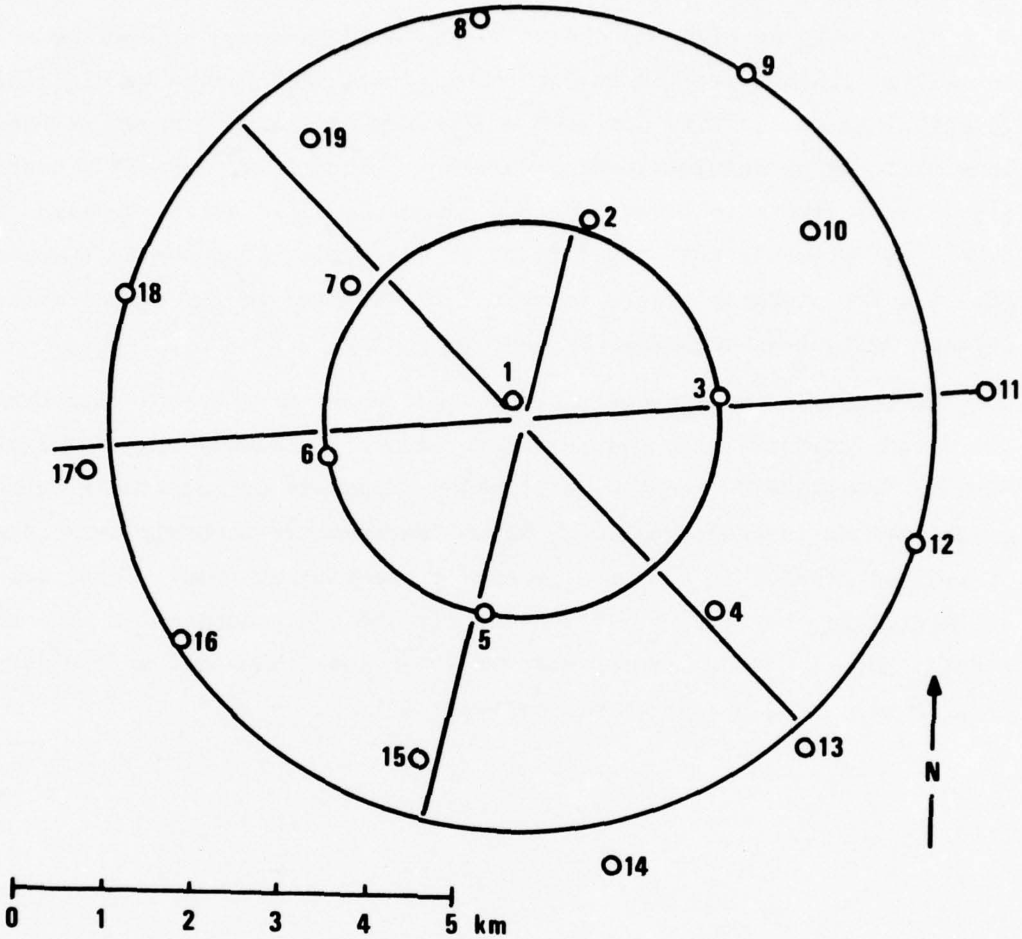

Figure 1. Korean short-period array.

The data quality was highly variable with about one-fourth of the tapes showing as many as eight to twelve channels inoperative or not operating normally. Another problem in data quality was the inadequate digitizing (quantizing) sensitivity for very small signals (noise samples in particular). This produced an angular looking waveform plot and is probably a source of significant errors in power spectrum computation for noise samples. These errors are probably most significant at the higher frequencies (greater than 3Hz) and are probably tolerable at the frequencies of importance in teleseismic work, less than 2Hz.

In addition to inadequate quantizing levels many traces also show distorted waveforms with jumps between several "plateaus" and peculiar looking "one-sided" traces with clipping, dropouts or non-linear compression of amplitudes in one direction. These features are probably associated with functional defects in the on-site data processing systems. There are segments of recordings, however, where the signals and background noise look completely normal. We estimate, however, that less than half of the data is free of some kind of system distortion.

NOISE SAMPLES

Six 320-second noise samples were analyzed to determine the Korean short-period noise characteristics. All noise samples preceded strong events selected by inspecting seismograms to be certain that all 19 seismometers were operating normally. All samples ended about ten seconds before the impulsive start of a clear first arrival P-phase close to the predicted arrival time.

Power spectra of six noise samples are shown in Figure 2. On the top part of the figure the spectra with the highest and lowest absolute noise level are shown. The largest difference between the two curves is about 4 to 5 dB. The lower part of the figure shows the rest of the spectra staggered on the vertical scale to avoid visual crowding. All spectra fall of sharply towards higher frequencies, and show secondary peaks at approximately 2 and 3Hz.

Reduction in noise spectra after beamforming is shown in Figures 3 and 4 for both the Korean and NORSAR comparable arrays. In the case of the NORSAR site the spectral data are "Average Subarray Beam" (Barnard and Whitelaw, 1972, Figure II-2). In both cases, spectral noise reduction is about equal to the square-root of the number of sensors (10 log N for power spectrum).

An analysis of the variation of spectral noise reduction was done for the six noise samples and several different azimuths, and velocities as listed in Table 3. The results are summarized in Figure 5. All fifteen cases listed in Table 3 were considered at each frequency and the median, minimum and maximum were calculated. It is clear from inspection of Figure 5 that beamforming noise reduction produced a median value within one dB of square root of N from 1.0 to 2.0Hz. From about 0.5 to 1.0Hz the median was better than square root of N by 3 to 5 dB. The average improvement over $N^{1/2}$ in the .9 to 1.5Hz range, which is of prime interest in teleseismic

---

Barnard, T. E. and Whitelaw, R. L., 1972, Preliminary evaluation of the Norwegian short-period array, Extended Array Evaluation Program Report No. 6, Texas Instruments Incorporated, Dallas, Texas.

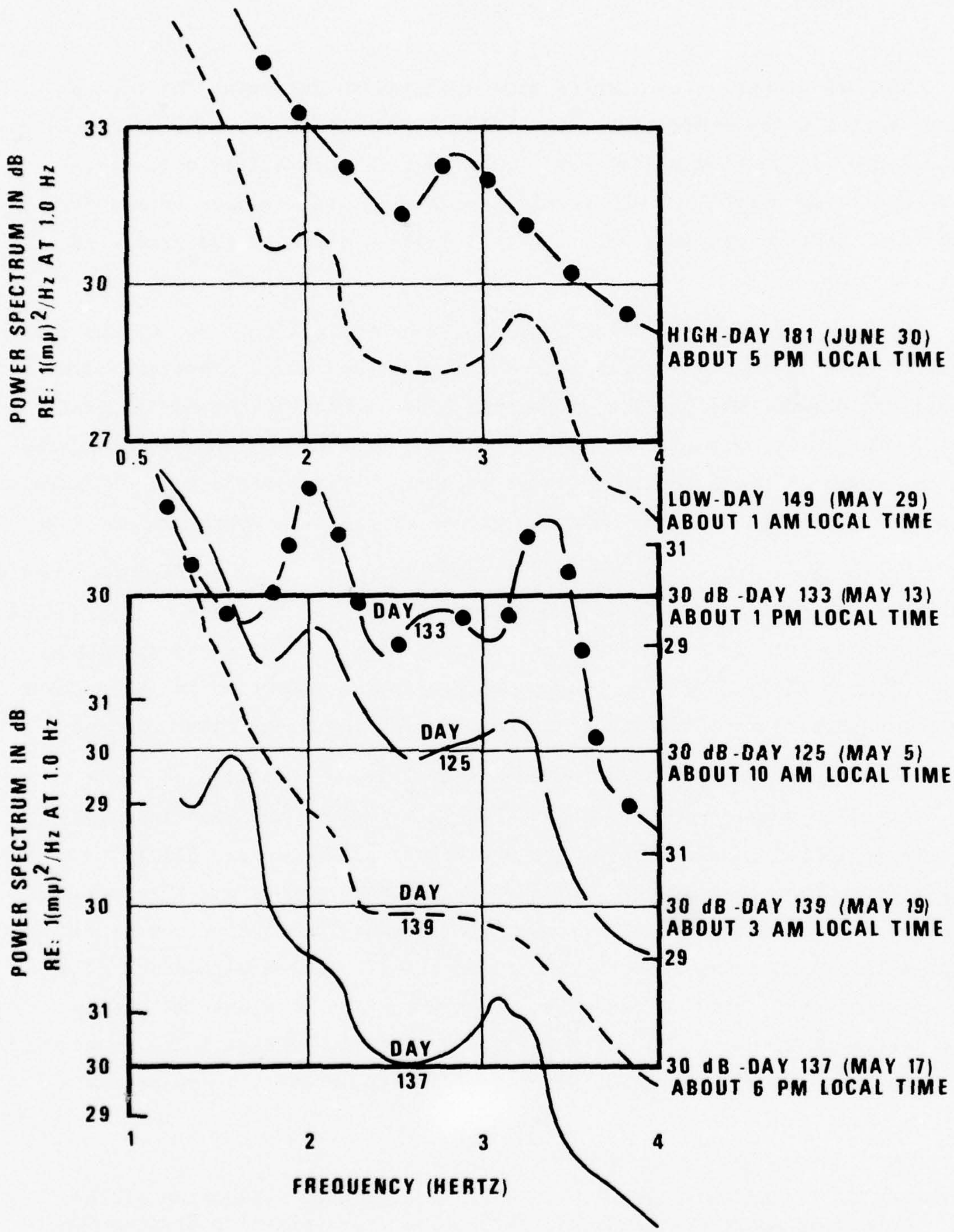

Figure 2. Variation of noise spectrum with frequency and date.

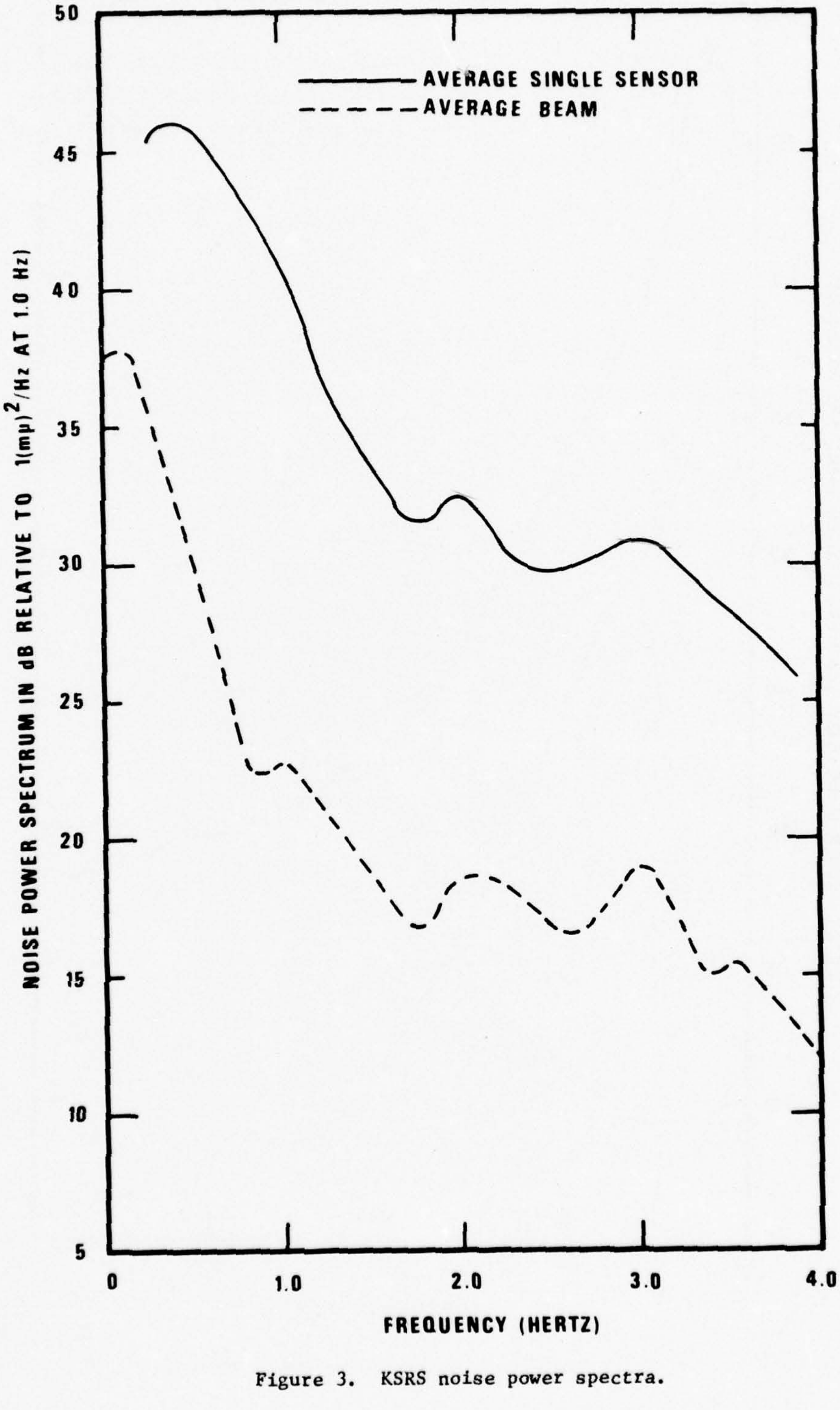

Figure 3. KSRS noise power spectra.

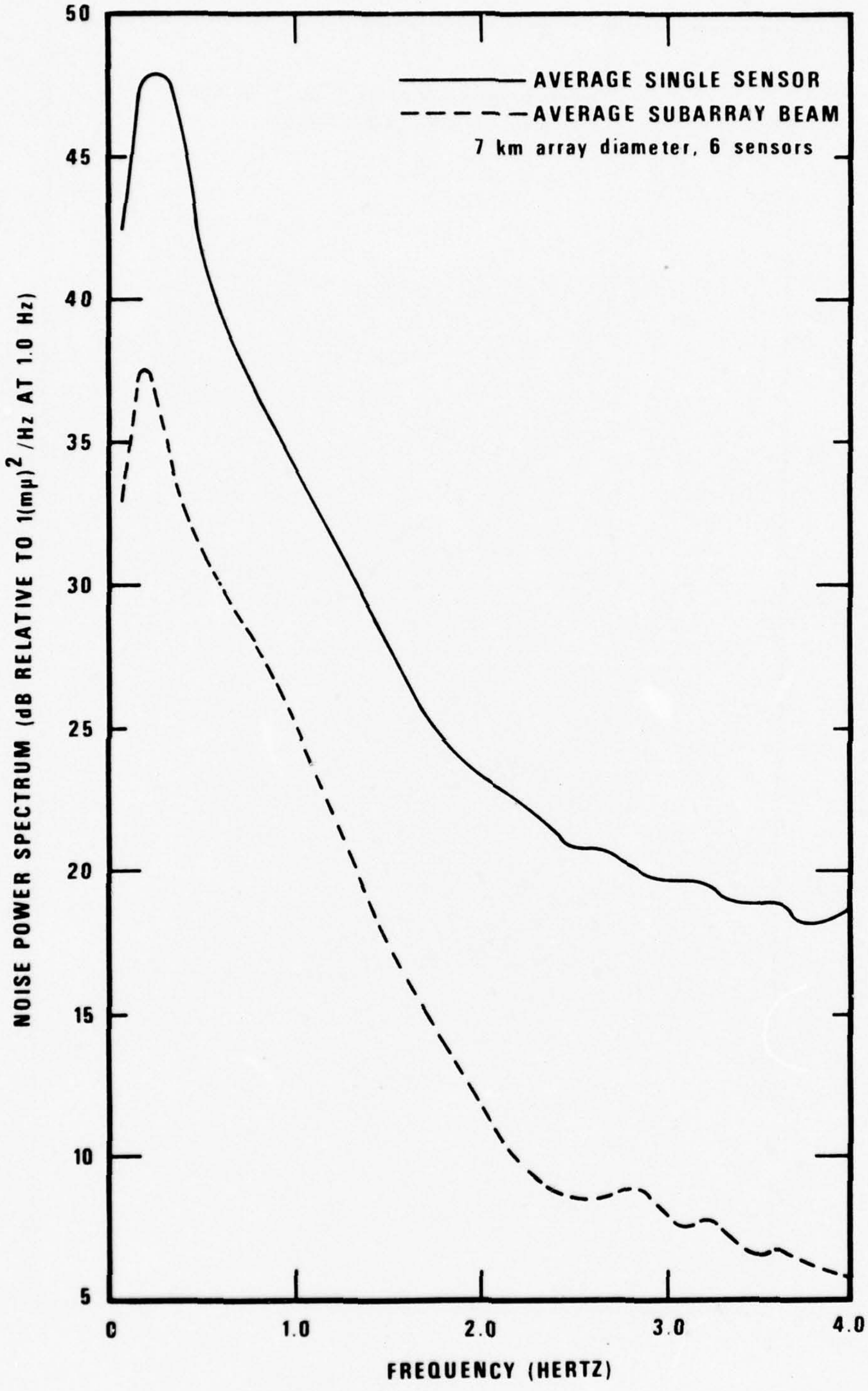

Figure 4. NORSAR noise power spectra.

TABLE III

KSRS Array Beams Used in Noise Analysis

DATE	VELOCITY (KM/SEC)	AZIMUTH (DEGREES)
May 05	Infinite	--
May 05	14	0
May 05	14	90
May 05	14	180
May 13	9	0
May 13	14	0
May 13	14	180
May 13	Infinite	--
May 17	Infinite	--
May 17	9	0
May 17	14	0
May 19	Infinite	--
May 19	14	0
May 29	Infinite	--
June 30	Infinite	--

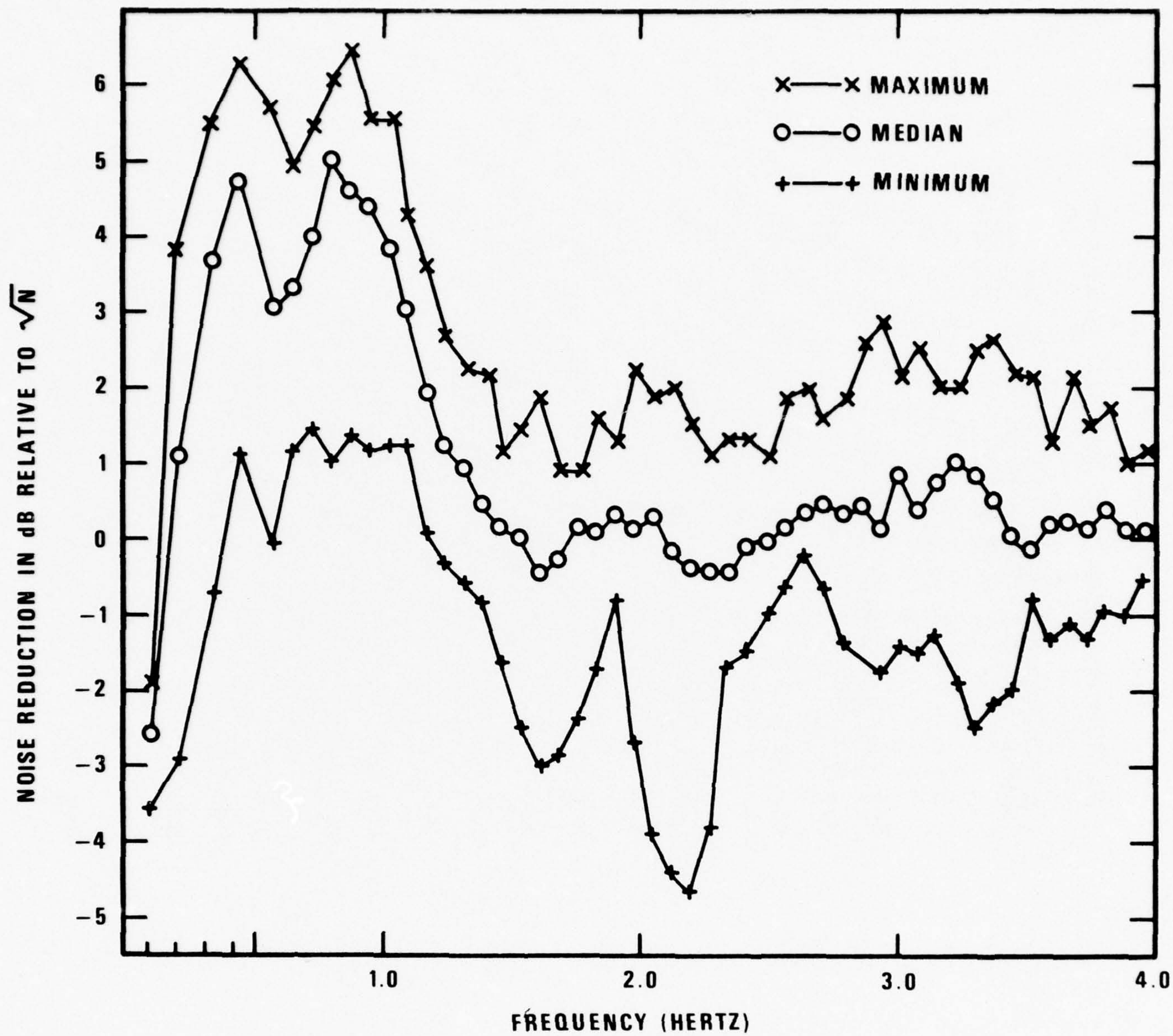

Figure 5. Distributions of spectral noise reduction after beamforming.

P-wave studies, is about 2 dB. The probable explanation for this effect also found by Prahl et al. (1975), is the presence of coherent propagating noise which is often present at coastal stations. As an independent check we also computed the noise reduction from estimates of array cross power spectral matrices and found identical results. The noise reduction is approximately the same for all velocities appropriate to teleseismic P waves. This is not surprising since the delays involved are small compared to the phase delays of slowly propagating 0.5-1.0Hz surface waves. At frequencies lower than .3Hz the long-period noise interferes constructively over the whole array.

Prahl, S. R., Shen, W. W., Whitelaw, R. L., 1975, Preliminary evaluation of the Korean seismological research station short-period array, Texas Instruments ALEX (01)-TR-75-05, Alexandria, Virginia.

PREFORMED BEAM DETECTION

Searches were made in predicted time windows for P-phases using the seven beams which are calculated by the station processor. The beam data channels are as indicated in Table 4.

As a result 114 detections were made from a total NEIS list (Table 2) of 209 events. Table 5 summarizes all 114 detections, giving date, abbreviated geographic region, seismic region, amplitude (in units based on the same conversion constant, 0.488 mμ/count, used for seismometer amplitude) and period. For the purpose of detectability calculation, the data were divided into two groups. The first group includes those events that were within the preformed beam azimuthal windows and the second group includes those events that were in the two azimuth gaps not covered by the preformed beam (080°-100° and 185°-205°) and events at distances greater than 100 degrees. The magnitudes were reduced to the epicentral distance of 60° and sorted into magnitude increment ranges. A maximum likelihood procedure described by Ringdahl (1976) was used to fit a detection probability curve to the observed probabilities of detection derived from Table 2. The results are given in Table 6 and Figure 6. The classification of one event of magnitude 6 was changed from undetected to detected since the failure to detect this event was due to malfunction in the recording system and it would have certainly been detected otherwise.

The body-wave detection thresholds together with their 95% confidence intervals for on-beam events at $\Delta = 60°$ were $5.42 \pm .45$ at the 90% level and $4.35 \pm .45$ at the 50% level. The detection thresholds of "all events" and off-beam events are within two standard deviations of this value; therefore, they are not significantly different. The 50% detection thresholds agree well with that derived by Texas Instruments group (Prahl, Shen, and Whitelaw, 1975). The 90° threshold is considerably higher than at other arrays

---

Ringdahl, F, 1976, On the estimation of seismic detection thresholds, Bull. Seism. Soc. Am., v. 65, p. 1631-1642.

TABLE IV

Preformed Beams

Channel #	Azimuth (Degrees)	Velocity (km/sec)
32	030	13.0
33	150	13.0
34	240	13.0
35	270	13.0
36	300	13.0
37	330	13.0
38	360	13.0

TABLE V

Detections from NEIS Bulletin
(114 out of Possible 209)

DATE	DAY (Julian Calendar)	EVENT # (Table 2)	GR/SR	AMP/PER	# OF GOOD SEIS.
4/29	119	1	HON/01	18/2.0	19
		2	BAN/01	60/1.5	19
		3	PHI/02	24/1.3	19
		4	PAN/04	35/1.1	19
		7	HDK/08	23/2.0	19
5/05	125	15	SOL/02	430/1.2	19
		19	IRA/06	130/0.9	19
		20	HON/08	110/0.5	19
		23	HOK/09	38/1.4	(19)
5/13	133	28	ASC/02	38/1.5	19
		29	BON/05	100/1.0	19
5/17	137	36	KUR/06	95/0.8	19
		37	SIN/10	240/1.2	19
5/19	139	38	MAR/18	48/0.8	19
		39	PER/19	310/1.2	19
5/21	141	40	CAR/12	40/0.9	(19)
5/25	145	44	WPA/09	90/1.5	19
		46	ORE/12	35/1.0	19
		47	ALA/13	194/0.9	19
5/29	149	51	MAS/12	57/1.2	19
		52	SSI/13	30/0.8	(19)
		54	BAF/16	22/1.0	(19)
		55	PBB/17	125/1.0	19
5/31	151	56	SUM/12	50/0.8	19
		58	RAT/18	112/0.8	19
6/02	153	59	IRA/14	32/0.8	18
6/04	155	60	PHI/10	34/0.9	18
		61	NBR/13	39/1.0	18
		62	ECU/13	20/0.8	18

TABLE V (Continued)

Detections from NEIS Bulletin
(114 out of Possible 209)

DATE	DAY (Julian Calendar)	EVENT # (Table 2)	GR/SR	AMP/PER	# OF GOOD SEIS.
6/06	157	67	NEV/13	2200/0.8	7
		69	SOL/14	150/1.0	14
		70	HIN/16	39/0.6	14
		71	CEL/17	34/1.2	19
6/08	159	74	BON/12	65/0.8	7
		75	NGU/14	65/0.7	7
6/10	161	80	CEL/16	46/1.0	(19)
		82	CAR/17	47/1.3	(19)
		83	GUA/18	36/1.5	(19)
6/12	163	85	SOL/12	150/1.0	3
		86	KAM/14	570/0.8	7
		87	HOK/15	386/0.8	6
6/14	165	89	FLO/11	1450/1.2	(19)
		90	SEV/13	20/0.4	(19)
		91	SUM/15	123/0.9	(19)
6/16	167	95	BKL/12	104/1.2	14
		97	ORE/15	495/1.5	14
		98	BAN/15	130/0.6	14
6/18	169	99	HOK/13	60/1.0	
		100	KUR/14	40/0.9	8
		101	KUR/15	66/1.2	11
		104	HOK/18	315/1.0	14
6/20	171	105	HON/15	38/0.8	(19)
		107	KER/18	115/0.8	19
6/22	173	108	FIJ/17	95/1.3	19
		110	NHE/18	26/1.1	(19)
		111	MAR/19	1807/0.8	19
		112	TON/20	414/1.4	19
6/24	175	114	MAR/17	400/2.0	19
		115	KUR/18	58/0.8	(19)
		116	NGU/18	81/1.4	(19)
		117	KUR/19	133/1.2	19
		118	KUR/20	238/1.5	19
		119	NOR/21	54/2.6	19
6/26	177	122	KUR/18	426/1.0	19
		123	HOK/18	84/1.0	(19)
		124	CRE/19	193/1.0	19

TABLE V (Continued)

Detections from NEIS Bulletin
(114 out of Possible 209)

DATE	DAY (Julian Calendar)	EVENT # (Table 2)	GR/SR	AMP/PER	# OF GOOD SEIS.
6/28	179	126	SCR/14	412/1.0	19
		127	MOL/15	58/1.0	19
		128	CHI/15	36/2.8	(19)
		130	NGU/17	75/1.1	19
		131	NEV/19	39/1.0	(19)
		133	BAN/20	138/1.2	19
6/30	181	134	GUA/08	84/1.2	(19)
7/02	183	141	AEG/12	22/1.0	(19)
		142	TAD/13	38/1.0	19
		143	ALA/14	32/0.9	19
		145	KAM/15	25/0.8	19
7/04	185	148	ALA/13	30/0.7	19
		150	ICB/17	34/1.0	(19)
		151	HON/17	65/0.9	19
7/06	187	152	NIC/05	23/0.9	19
		154	CBB/07	13/0.8	(19)
		155	CHI/04	58/1.5	19
		156	CHI/11	11/0.8	(19)
		157	CHI/12	23/2.0	19
7/08	189	159	OKH/15	76/0.6	(19)
		160	LEE/17	38/1.3	19
		161	CHI/18	47/1.4	19
7/10	191	163	CHI/15	47/2.0	19
		165	KUR/18	31/1.2	19
7/12	193	169	CHI/14	100/2.2	19
		170	CHI/15	15/1.0	(19)
		171	CHI/16	67/1.5	19
		172	CHI/16	106/1.4	19
		173	PHI/19	55/1.0	19
7/14	195	174	GRE/13	60/0.7	19
		175	TIB/14	326/1.8	19
7/16	197	176	FLO/13	55/1.6	19
		178	MEX/18	31/1.1	19
		179	TIB/20	277/1.2	19
7/20	201	183	CER/10	49/1.6	17
7/22	203	188	SSI/15	12/1.0	10
		189	KER/15	11/1.0	10
		190	PHI/15	28/0.8	(10)
		193	HON/18	23/1.2	10

TABLE V (Continued)

Detections from NEIS Bulletin
(114 out of Possible 209)

DATE	DAY (Julian Calendar)	EVENT # (Table 2)	GR/SR	AMP/PER	# OF GOOD SEIS.
7/24	205	197	KUR/15	98/1.1	(10)
		198	SOL/15	44/1.2	(10)
		199	CHI/20	264/1.3	10
7/26	207	202	MAC/14	45/1.5	13
		203	AND/14	62/1.2	13
		205	AND/15	26/1.1	13
		207	AND/19	91/1.2	13
		208	AND/20	49/1.5	13
		209	AND/20	401/1.2	13

TABLE VI

Incremental Detection Ratios

Mag. Range (Center Value)	All Events	Events In Preformed Beams	Events Outside Preformed Beams
3.6	.00	.00	--
3.8	.29	.33	.00
4.0	.43	.75	.00
4.2	.53	.71	.00
4.4	.31	.29	.33
4.6	.58	.54	.71
4.8	.60	.59	.63
5.0	.86	.83	1.00
5.2	.88	.83	1.00
5.4	.93	1.00	.87
5.6	.91	1.00	.75
5.8	1.00	1.00	1.00
6.0	1.00*	1.00*	--
6.2	1.00	1.00	--

* Changed from .5 to 1.0 justification in text

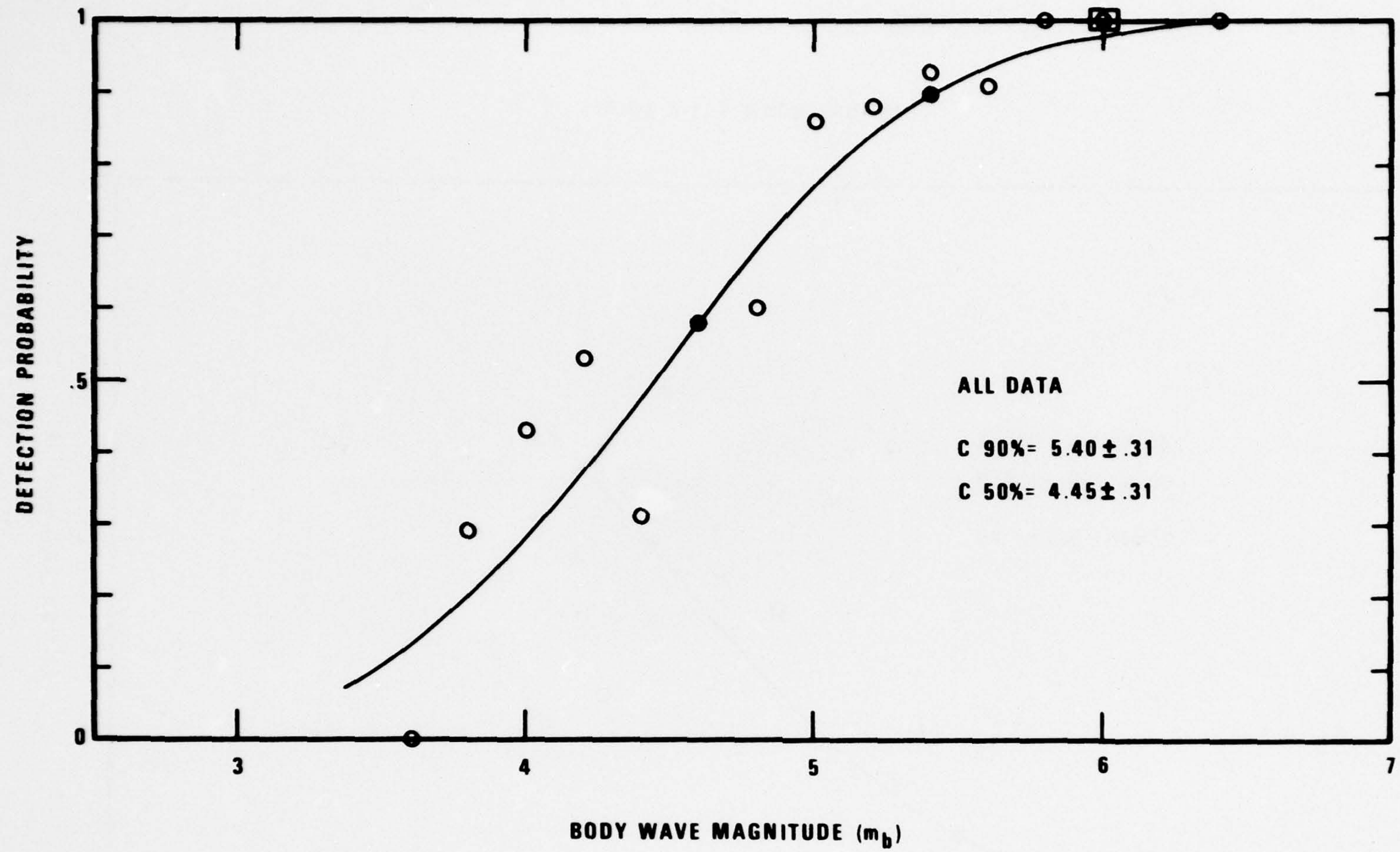

Figure 6. Observed incremental detection probabilities and the maximum likelihood detection probability curve fitted to data. Filled circles show the 50% and 90% detection levels.

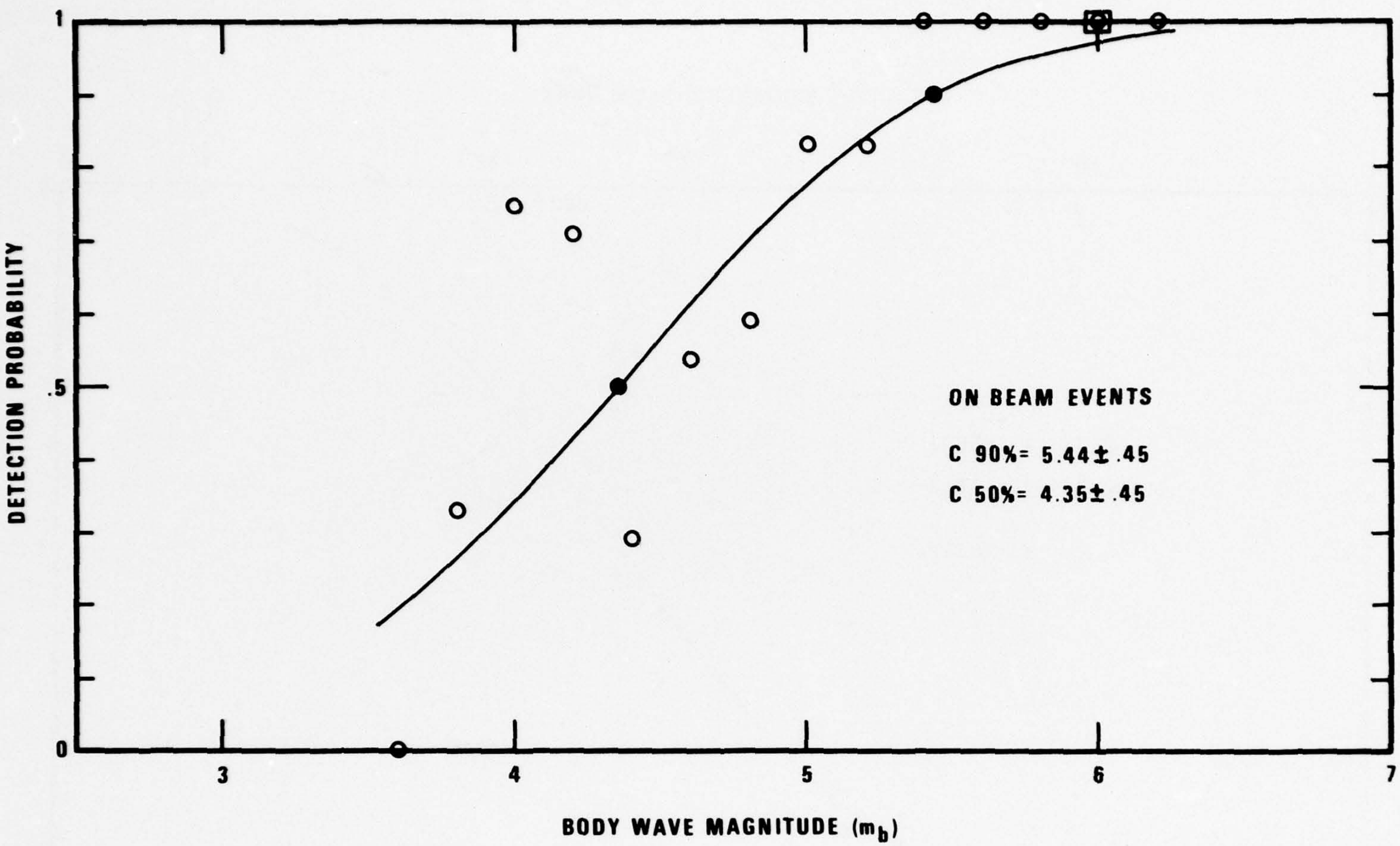

Figure 6 (Continued). Observed incremental detection probabilities and the maximum likelihood detection probability curve fitted to data. Filled circles show the 50% and 90% detection levels.

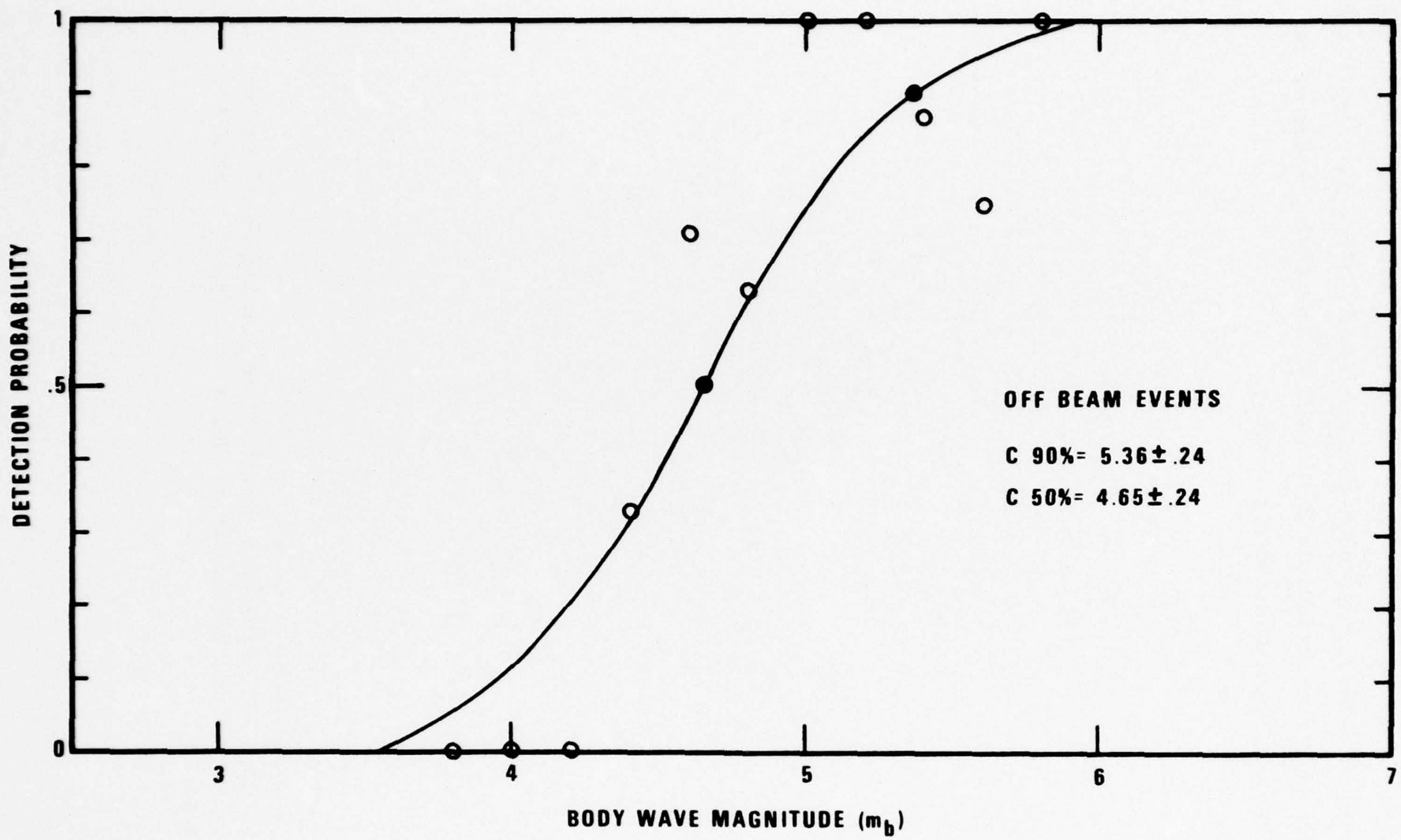

Figure 6 (Continued). Observed incremental detection probabilities and the maximum likelihood detection probability curve fitted to data. Filled circles show the 50% and 90% detection levels.

(Dean, 1971; Barnard and Whitelaw, 1972). One can attribute this to the high noise level at KSRS which is about three times the average noise amplitude at NORSAR. Although data quality is often poor, only a few events were not detected because of instrument malfunctions; these do not effect the threshold determination appreciably.

Dean, W. C., 1971, Detection threshold fo the LASA/SAAC system, Seismic Array Analysis Center Report No. 3, Teledyne Geotech, Alexandria, Virginia.

UNFILTERED SIGNAL BEAMFORMING

Fifteen of the best events were selected for unfiltered signal and noise beamforming in the precalculated direction and azimuth of the event. In Table 7 we give the signal loss at beaming and the average wide-band noise reduction in dB. The results show that the signal loss is very small indicating that the signal is similar across the array. The overall noise amplitude reduction is close to $\sqrt{N}$ (12.8 dB). This is probably because the noise cancellation in wide band use is dominated by noise amplitudes at the spectral peak where at the low frequency side the noise reduction is worse than $\sqrt{N}$ while at slightly higher frequencies it is better (see Figures 3 and 5), the overall result is therefore close to $\sqrt{N}$.

TABLE VII

Beamforming to Selected Events

EVENT	AZ.	VEL.	SIGNAL LOSS dB	NOISE REDUCTION dB
SOL/125/02	143.5	15.16	0.45	11.48
IRA/125/06	288.6	15.62	0.85	12.18
BON/133/05	130.1	10.32	0.39	10.70
KUR/137/06	059.4	8.95	1.35	14.37
SIN/137/10	290.2	12.90	0.31	12.73
PER/139/19	047.2	79.76	0.57	13.78
ALA/145/13	047.8	14.70	0.25	12.38
PBB/149/17	039.9	72.16	1.09	14.55
RAT/151/18	052.0	13.02	0.46	10.10
TON/173/20	126.6	20.56	0.19	14.90
MAR/175/17	137.0	10.32	0.33	8.99
KUR/175/20	062.2	8.53	1.00	10.70
SCR/179/14	136.1	16.62	0.26	12.73
TIB/195/14	279.0	12.72	0.02	13.26
TIB/197/20	278.7	12.75	0.71	9.22

SUMMARY

Evaluation of the Korean Seismic Research Station led to the following conclusions.

1.) The average wide band rms noise reduction is about 2 dB better than $\sqrt{N}$ due to coherent propagating noise at frequencies below 1.5Hz. At frequencies above 1.5Hz the noise is incoherent.

2.) The 50% body wave detection threshold is at $m_b = 4.35 \pm .45$ at the epicentral distance of 60°. The 90% detection threshold is at $m_b = 5.42 \pm .45$. The limits indicated above are at the 95% confidence level.

3.) Instrument and system malfunctions reduce the utility and reliability of the data at this array in the May - June 1973 time interval greatly.

REFERENCES

Barnard, T. E. and Whitelaw, R. L., 1972, Preliminary evaluation of the Norwegian short-period array, Extended Array Evaluation Program Report No. 6, Texas Instruments Incorporated, Dallas, Texas.

Dean, W. C., 1971, Detection threshold of the LASA/SAAC system, Seismic Array Analysis Center Report No. 3, Teledyne Geotech, Alexandria, Virginia.

Prahl, S. R., Shen, W. W., and Whitelaw, R. L., 1975, Preliminary evaluation of the Korean seismological research station short-period array, Texas Instruments ALEX (01)-TR-75-05, Alexandria, Virginia.

Ringdahl, F., 1976, On the estimation of seismic detection thresholds, Bull. Seism. Soc. Am., v. 65, p. 1631-1642.